

Quantum dynamics using path integral coarse-graining

Félix Musil,¹ Iryna Zaporozhets,^{1,2,3} Frank Noé,^{1,3,2} Cecilia Clementi,^{1,3,2,*} and Venkat Kapil^{4,†}

¹*Department of Physics, Freie Universität Berlin, Arnimallee 12, 14195 Berlin, Germany*

²*Department of Chemistry, Rice University, Houston, Texas 77005, United States*

³*Center for Theoretical Biological Physics, Rice University, Houston, Texas 77005, United States*

⁴*Yusuf Hamied Department of Chemistry, University of Cambridge, Lensfield Road, Cambridge, CB2 1EW, UK*

Vibrational spectra of condensed and gas-phase systems containing light nuclei are influenced by their quantum-mechanical behaviour. The quantum dynamics of light nuclei can be approximated by the imaginary time path integral (PI) formulation, but still at a large computational cost that increases sharply with decreasing temperature. By leveraging advances in machine-learned coarse-graining, we develop a PI method with the reduced computational cost of a classical simulation. We also propose a simple temperature elevation scheme to significantly attenuate the artefacts of standard PI approaches and also eliminates the unfavourable temperature scaling of the computational cost. We illustrate the approach, by calculating vibrational spectra using standard models of water molecules and bulk water, demonstrating significant computational savings and dramatically improved accuracy compared to more expensive reference approaches. We believe that our simple, efficient and accurate method could enable routine calculations of vibrational spectra including nuclear quantum effects for a wide range of molecular systems.

Predictive simulations of thermodynamic and time-dependent properties of condensed and gas-phase systems lay the foundations of computational materials design and discovery.¹ Accurate modeling of many systems, such as those containing light nuclei like H, C, N, and O, must account for their quantum-mechanical behavior to include the zero-point motion of collective modes² and the tunneling of the system across classically inaccessible barriers.³ Phenomena emerging from the quantum dynamics of light nuclei are ubiquitous in chemistry and material science of molecular systems, for instance, the relative diffusion of H₂ in clathrate hydrates⁴ and kinetic isotope effects in porous organic crystals,⁵ proton-transfer rates in molecular switches,⁶ the red-shift in the IR spectra of O–H stretch mode in ice⁷ and the characterization of (bio-)molecular systems using vibrational spectroscopy.⁸

Unfortunately, the exact description of quantum dynamics – requiring the solution of Schrödinger’s equation – is possible only for the smallest of systems, such as molecules containing a few atoms.^{9,10} Extension to larger systems requires “local” approximations or truncation of the interaction potential and/or an approximate solution of the many-body Schrödinger equation,^{11–13} akin to the electronic structure problem. Alternatives that render an “approximate but full” quantum-mechanical treatment of all degrees of freedom are based on the (semi-)classical dynamics of the system.¹⁴ In this context, imaginary time path integral (PI) simulations, although originally formulated for incorporating the quantum statistical effects,¹⁵ are becoming increasingly popular for studying the approximate quantum dynamics of distinguishable particles.¹⁴ State-of-the-art PI approaches^{16–19} neglect

real time quantum coherence but include effects arising from the quantum statistical distribution of the nuclei.²⁰ These methods give a good description of the dynamical response of condensed phase systems, for instance, vibrational spectra of bulk water²¹ and ice,¹⁹ where quantum coherence effects last only over short times. On the other hand, predicting the vibrational response of molecules and clusters is still a challenge, the reasons being twofold. Firstly, the artifacts of PI methods (arising from the neglect of real-time coherence and approximations to non-centroid Matsubara fluctuations²²), such as spurious broadening and frequency shifts of quantal modes, become worse with a reduction in temperature.²³ Secondly, the computational cost of PI methods increases steeply with inverse temperature²⁴ making them expensive to obtain a direct comparison with experiments. In the last few decades, many new approaches have aimed at individually improving the accuracy^{25–28} or efficiency^{19,29–31} of PI dynamical methods. These studies highlight the urgency for an accurate, efficient, and generally-applicable method that can treat the quantum dynamics of molecules, clusters, and bulk systems at the same footing, and aid in modeling their vibrational response.

In this work, we combine PI and coarse-graining methods via machine learning to render the calculation of quantum vibrational spectra accurate and computationally affordable and demonstrate its capabilities on paradigmatic aqueous systems. Our approach builds upon the state-of-the-art centroid molecular dynamics¹⁶ (CMD) approach, which time-evolves the system *classically* on the free energy surface (FES) of the centroid of the imaginary time path – a modified PES that includes nuclear quantum effects. Its two key features, a temperature elevation (T_e) *ansatz* and path integral coarse-graining simulations (PIGS), ensure accuracy and computational efficiency. On one hand, the T_e *ansatz*

* cecilia.clementi@fu-berlin.de

† vk380@cam.ac.uk

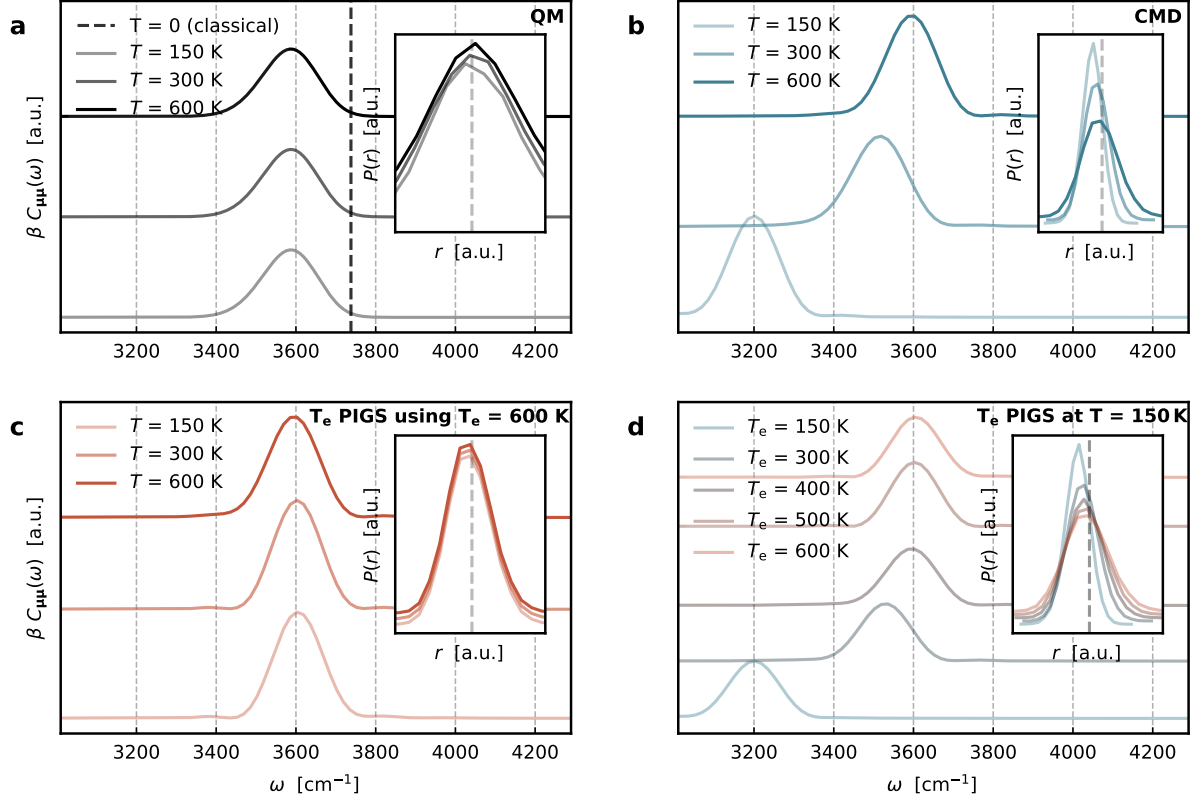


FIG. 1. **Temperature dependent IR spectrum of an O–H bond described by a Morse oscillator.** The IR spectrum of a 2D Morse oscillator mimicking an O–H at 600 K, 300 K, 150 K calculated by (a) solving the Schrödinger's equation numerically (QM),²⁸ and using (b) centroid molecular dynamics (CMD), and (c) T_e PIGS using $T_e = 600$ K. Panel (d) shows the dependence of the T_e PIGS IR spectrum on the temperature of the centroid free energy surface, (T_e). Insets shows the temperature dependent radial probability densities calculated using the respective methods and the dashed grey vertical line is the mode of quantum-mechanical distribution. Note that the range of y axes are not kept the same to aid clarity.

alleviate the spurious redshift in CMD, leading to an improvement in the accuracy of vibrational spectra over state-of-the-art methods. On the other hand, with PIGS we machine learn the centroid FES in a general manner, i.e., without making prior assumptions about the functional form of the system's PES, and use it to evolve the system classically. This method, referred to as T_e PIGS, enables the calculation of the IR spectra of aqueous systems including nuclear quantum effects, in excellent agreement with numerically exact or more expensive reference methods. Furthermore, we demonstrate that our approach is transferable across phases and temperatures allowing modeling of vibrational spectra at *cryogenic* temperatures at orders of magnitude lower computational cost using classical MD.

We first discuss CMD and introduce T_e PIGS in the context of a simple yet realistic anharmonic system that highlights the deficiencies of PI methods at low temperatures: a 2D radial Morse oscillator mimicking an O–H

bond, described by the Hamiltonian,

$$\hat{H} = (2\mu)^{-1} [\hat{p}_x^2 + \hat{p}_y^2] + D \left[1 - e^{-\alpha(\sqrt{\hat{q}_x^2 + \hat{q}_y^2} - r_0)} \right]^2, \quad (1)$$

where the parameters μ , D , α , and r_0 are defined in section I.A of the supporting information (SI). The O–H bond has a large zero point energy $E_0 \approx 1843 \text{ cm}^{-1} \approx 2652 \text{ K}$ and a $0 \rightarrow 1$ transition energy $E_1 - E_0 \approx 3568 \text{ cm}^{-1} \approx 5134 \text{ K}$ (see section I.A of the SI for more details), meaning that even at a temperature of 600 K the system resides almost exclusively in its ground state, yet probes anharmonic regions of the PES due to zero-point motion. As shown in Fig. 1(a), this results in a temperature-independent line position of the IR spectrum, at least up to 600 K, but also a red-shift of around 200 cm^{-1} with respect to the classical spectrum due to quantum nuclear motion.

The CMD approach¹⁶ is based on the imaginary time path integral isomorphism³² between the thermodynamics of a quantum system at inverse temperature β and a classical ring polymer made of P replicas of the system

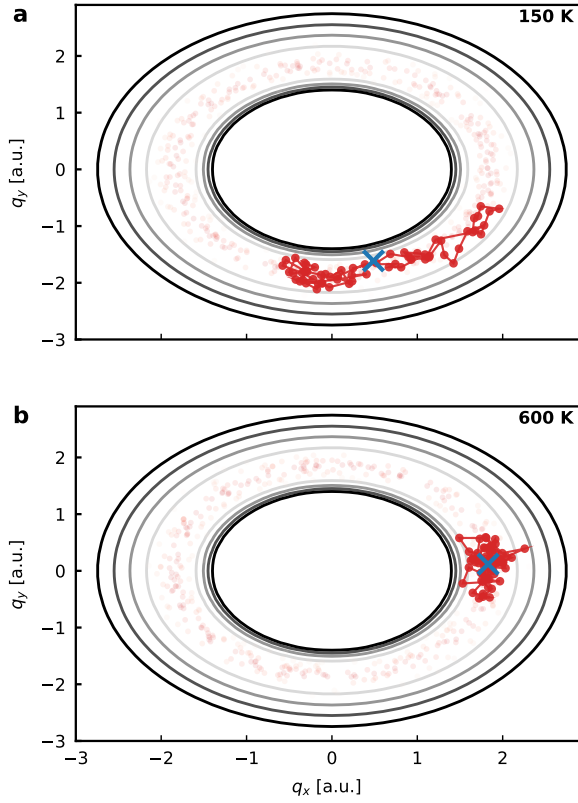


FIG. 2. The curvature problem in centroid molecular dynamics. Contour plots of a 2D Morse radial potential up to half the dissociation energy (black to grey solid lines), the probability density of the system (red to white indicating high to low), and a snapshot of the ring polymer (red) and its centroid (blue) at (a) 150 K and (b) 600 K.

at $\beta_P = \beta/P$,

$$Z = \text{Tr}[e^{-\beta \hat{H}}] \propto \lim_{P \rightarrow \infty} \int d\mathbf{q} e^{-\beta_P [\sum_j U(\mathbf{q}^{(j)}) + U^{\text{spr}}(\mathbf{q})]}, \quad (2)$$

where $\mathbf{q} \equiv \{\mathbf{q}^{(1)}, \dots, \mathbf{q}^{(P)}\}$ is a shorthand for positions of the P replicas of the system with $\mathbf{q}^{(j+P)} \equiv \mathbf{q}^{(j)}$ implied, $U(\mathbf{q})$ defines the classical PES, and $U^{\text{spr}}(\mathbf{q})$ is a temperature dependent spring term³² that connects consecutive replicas of the system. Within CMD, the system is time evolved *classically* on $U^{\text{CMD}}(\mathbf{q}_c; \beta)$, defined as the free energy surface of the centroid of the imaginary time path (modulo a constant) at β ,

$$U^{\text{CMD}}(\mathbf{q}_c; \beta) = -\beta^{-1} \log \left\langle \delta \left(\frac{1}{P} \sum_{j=1}^P \mathbf{q}^{(j)} - \mathbf{q}_c \right) \right\rangle_\beta, \quad (3)$$

where $\sum_{j=1}^P \mathbf{q}^{(j)}/P$ is the centroid of the ring polymer and $\langle \cdot \rangle$ an average over the path integral Hamiltonian in Eq. 2. The thermodynamic force acting on the centroid can be calculated *on the fly* from a constrained PI

simulation at each CMD step¹⁶

$$\begin{aligned} \mathbf{f}^{\text{CMD}}(\mathbf{q}_c; \beta) &= -\nabla U^{\text{CMD}}(\mathbf{q}_c; \beta) \\ &= \left\langle \mathbf{f}_c \delta \left(\frac{1}{P} \sum_{j=1}^P \mathbf{q}^{(j)} - \mathbf{q}_c \right) \right\rangle_\beta, \end{aligned} \quad (4)$$

where, $\mathbf{f}_c = \sum_{j=1}^P \mathbf{f}^{(j)}/P$, and $\mathbf{f}^{(j)}$ is the physical force acting on the j -th replica. Alternatively, the centroid can be evolved on its FES within a PI simulation in a partially adiabatic manner³³ by decoupling the centroid from the rest of the system. Dynamical properties, such as the IR spectrum, can be easily calculated via classical time correlation functions (TCFs) on the basis of the centroid trajectory, akin to classical MD.

As shown in Fig. 1(b), the IR spectrum of the O–H bond computed with CMD is in excellent agreement with the numerically exact result at 600 K. Unfortunately, at lower temperatures, the system experiences a spurious red shift that gets worse as the temperature is reduced. This well-known artifact is referred to as the “curvature problem”²³ and arises in cases where the ring polymer has a shape such that its centroid lies outside the ring (see Fig. 2) and therefore does not represent the quantum-mechanical probability density of the system (as obtained by the replicas). Interestingly, the curvature problem is purely a structural artifact, and, as shown in the inset of Fig. 1(b), it can be diagnosed from PI trajectories: the misalignment of the distribution of the centroid at 300 K and 150 K to the (physical) probability density obtained from the replicas. As mentioned above, another issue with CMD, and more generally with PI methods, is that the required number of replicas scales inversely with temperature and the maximum physical frequency of the system, $P \sim \beta \hbar \omega_{\text{max}}$.³⁴ Therefore its computational cost increases steeply as the temperature is reduced. These challenges prevent investigations of systems at cryogenic temperatures where most experimental data is available.

Recently, Trenins *et al.*^[28] have proposed a *quasi* centroid molecular dynamics (QCMD) scheme, that evolves the system on the FES of an *ad hoc* curvilinear function of replica positions – a *quasi* centroid that does not “fall out” of the hull of the path integral. A careful selection of this function doesn’t hamper quantum Boltzmann statistics and results in a compact PI ring polymer that alleviates the curvature problem. This results in an excellent agreement of the vibrational spectrum of a molecule of water, liquid water, and proton disordered hexagonal ice³⁵ with (numerically exact) reference methods. More recently, Fletcher *et al.*^[31] have proposed an efficient *fast* QCMD scheme that avoids the costly *on the fly* quasi-centroid forces by precomputing an analytic FES on the basis of a PI trajectory. This reduces the cost of predicting an accurate vibrational spectrum to that of classical MD,

resulting in an improvement over standard PI methods for the calculation of vibrational spectra of exemplary molecular systems.³¹ Unfortunately, the computational cost of these approaches still grows unfavorably with temperature due to the need for a low-temperature PI trajectory for fitting the FES. Moreover, an extension to general systems requires a general/universal procedure to fit the FES of the centroid and careful knowledge of appropriate curvilinear coordinates that do not suppress sampling of the physical regions of the configurational space.³⁶ Nonetheless, the advancements brought forth by (*fast*) QCMD^{28,31} suggest that further improvements in CMD provide a promising route towards the accurate and efficient calculation of vibrational spectra.

Taking inspiration from *fast* implementations of CMD³⁷ we propose path integral coarse-grained simulations (PIGS) that perform MD on a modified PES – including quantum nuclear effects. In particular, we leverage the recent developments in the definition of coarse-grained machine learning potentials^{38–40} and of high-order correlation functions^{41,42} to obtain this modified potential by coarse-graining the imaginary time path integral to that of a classical system. In this work, we use PIGS to accelerate CMD in a general manner, i.e. it is applicable to systems exhibiting a wide range of interparticle interactions. To obtain the centroid FES at β_e , we use the force matching method^{43,44} that is typically used to build thermodynamically consistent bottom-up coarse-grained models for macromolecular systems, i.e. the coarse-grained model reproduces the thermodynamic properties of the all-atom system projected onto the coarse-grained coordinates. It has been shown⁴⁴ that Eq. (3) can be recast as a variational principle: $U^{\text{CMD}}(\mathbf{q}_c; \beta)$ corresponds to the minimum of the force matching functional:

$$U^{\text{CMD}}(\mathbf{q}_c; \beta) = \arg \min_{G \in C(\mathbb{R}^n)} \left\langle \left\| \mathbf{f}_c + \nabla G(\mathbf{q}_c) \right\|^2 \right\rangle_{\beta}, \quad (5)$$

where the average is performed at inverse temperature β with the PI centroid constrained at $\mathbf{q}_c \in \mathbb{R}^n$, and the minimization is performed over the space $C(\mathbb{R}^n)$ of all real continuous functions $G : \mathbb{R}^n \rightarrow \mathbb{R}$. In this work we optimize a machine learning model as a surrogate for the potential of mean force to reproduce the thermodynamics of the centroid without having to explicitly simulate P replicas of the system. In practice, we only learn the difference between the centroid FES and the classical PES, as it is done in Ref.³⁷ This keeps the amount of training data to a minimum and provides an appropriate prior in the absence of data or for collective modes that do not exhibit quantum nuclear effects.

The centroid potential of mean force associated with an atomic configuration is expressed as a sum of the classical PES associated with U , and atom-centered contributions

$$\tilde{U}^{\text{CMD}}(\mathbf{r}; \boldsymbol{\theta}) = U(\mathbf{r}) + \sum_i A_{a_i}(\mathbf{r} - \mathbf{r}_i; \boldsymbol{\theta}), \quad (6)$$

where $\boldsymbol{\theta}$ is a set of model parameters, $\mathbf{r} \equiv \{\mathbf{r}_1, \dots, \mathbf{r}_N\}$ is a shorthand for set of atomic positions of a structure, \mathbf{r}_i is the position of the i^{th} atom of species a_i , and the A_{a_i} functions are parameterized using a machine learning model that captures the multi-body interactions emerging from the coarse-graining procedure.⁴⁵ We model the atomic potentials of mean force, A_{a_i} , by representing the atomic environment with the normalized SOAP powerspectrum^{46–48} and pass these 3-body features to a multi-layer perceptron with 3 hidden layers of width [400, 200, 200] and the hyperbolic tangent activation function. The parameters of the model are obtained by minimizing the force matching loss

$$\left\| \mathbf{f}_c + \nabla \tilde{U}^{\text{CMD}}(\mathbf{q}_c; \boldsymbol{\theta}) \right\|^2, \quad (7)$$

over a set of centroid sample forces \mathbf{f}_c and configurations \mathbf{q}_c obtained from a PIMD simulation at β performed with the **i**-PI code⁴⁹ (see section I.C of the SI for more details). The model and its training have been implemented in **pytorch**⁵⁰ and the codes are available upon request.

We propose a simple and physically motivated temperature elevation (T_e) *ansatz* that alleviates the curvature problem of CMD and also eliminates the unfavorable temperature dependence associated with the computational cost of vibrational spectra. We note that for a system in its ground state, i.e. $\hbar\omega \gg \beta^{-1}$, the IR spectrum – related by the dipole correlation function – is only *trivially* dependent on the temperature (see section II.A of the SI). It is easy to show that after rescaling with the inverse temperature β , the Kubo-transformed time-correlation function is a constant if the system is in its ground state, i.e., $\beta \tilde{C}_{\hat{\mu}\hat{\mu}}(\omega; \beta) = \text{constant}$. As shown in Fig. 1(b), CMD does not follow this behavior because of the curvature problem at low temperatures. To avoid this artifact, we propose a T_e *ansatz*, i.e. we rewrite a time-correlation function in terms of a CMD time-correlation function computed at an elevated temperature T_e , $\tilde{C}_{\hat{\mu}\hat{\mu}}^{T_e}(\omega; \beta; \beta_e) = \frac{\beta_e}{\beta} \tilde{C}_{\hat{\mu}\hat{\mu}}^{\text{CMD}}(\omega, \beta_e)$. We approximated it as

$$\tilde{C}_{\hat{\mu}\hat{\mu}}^{T_e}(\omega, \beta; \beta_e) \approx Z^{-1} \int d\mathbf{q}' e^{-\beta U^{\text{CMD}}(\mathbf{q}'; \beta_e)} \boldsymbol{\mu}(0) \cdot \boldsymbol{\mu}(t), \quad (8)$$

so that it is easily calculated by evolving the centroid at β on a FES calculated at a high temperature β_e . Eq. 8 is exact in the harmonic and classical limits, and it avoids the spurious red-shifts at low temperatures as the FES at β_e doesn't exhibit the curvature problem.

As shown in Fig. 1(b), the CMD IR spectrum remains in excellent agreement with the exact result at 600 K and the radial distribution function of the centroid of the O–H bond is aligned with the physical distribution. These observations suggest that the system doesn't

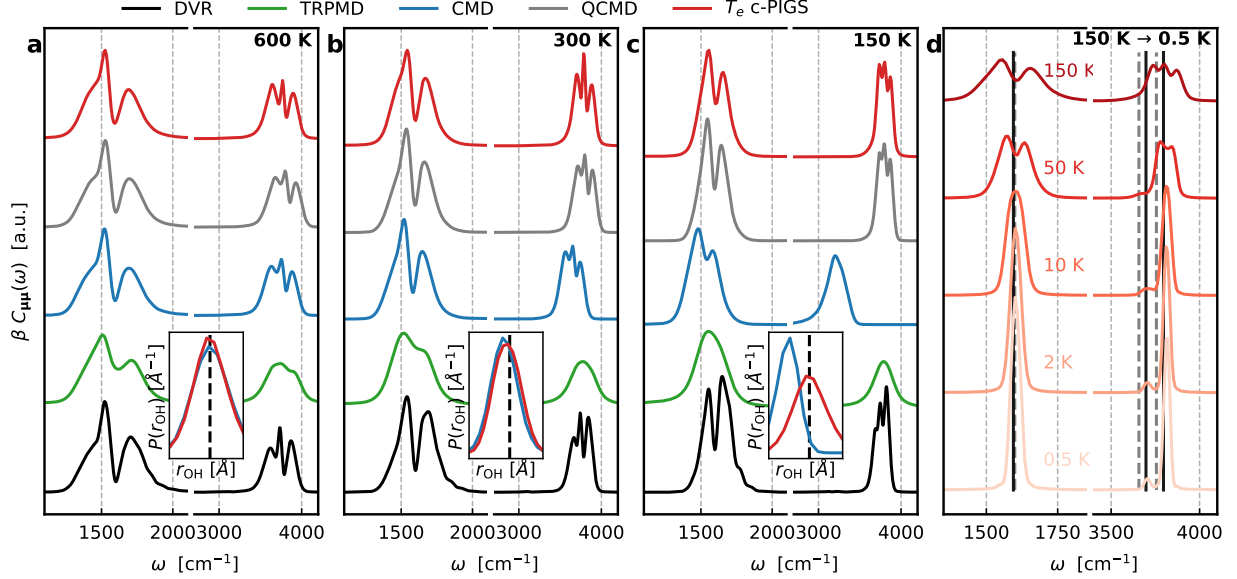


FIG. 3. **Quantum dynamics of a water molecule.** Comparison of the vibrational spectrum of a water molecule described by the Partridge-Schwenke model⁵¹ at (a) 600 K, (b) 300 K, (c) 150 K, using discrete value representation (yielding numerically exact results) in black, the proposed T_e PIGS approach using the centroid free energy surface calculated at 600 K in red, CMD in blue, and TRPMD in green. The insets show the probability distribution of the O-H bond length calculated from the CMD and T_e PIGS and the black dashed line indicates the mode of the distribution obtained from PIMD – constant across temperatures. Panel (d) displays the temperature-dependent IR spectrum of a water molecule from 600 K down to 0.5 K. The gray dashed line indicates the reference $0 \rightarrow 1$ transition frequency while the black line is shifted by 40 cm^{-1} to reflect the results obtained with Matsubara dynamics.²²

exhibit the curvature problem at 600 K and thus we test the T_e *ansatz* for $T_e = 600 \text{ K}$ where $\beta_e = (k_B T_e)^{-1}$. As shown in Fig. 1(c) and Fig. 1(d), increasing the “elevated temperature” progressively improves the description of the IR spectrum at 150 K. Moreover, using $T_e = 600 \text{ K}$ leads to an excellent agreement of the temperature dependent IR spectrum with the exact result. Note that for the Morse potential there exists a wide window of suitable T_e (see section II.B of the SI for more details), i.e. large enough to alleviate the curvature problem but also small enough for the harmonic approximation in Eq. 8 to be valid, and we observed similar features with the water molecule and bulk water. Fig. 1(c) shows that the line position of the predicted IR spectra and the radial distribution of the O-H bond are largely temperature independent using $T_e = 600 \text{ K}$, as expected for a system in its ground state. Finally, the number of replicas needed to calculate $U^{\text{CMD}}(\mathbf{q}'; \beta_e)$ is $P \approx \beta_e \hbar \omega_{\text{max}} < \beta \hbar \omega_{\text{max}}$ which is independent of β . Thus, within the T_e *ansatz*, the cost of simulating the quantum dynamics of a system in its ground state at β doesn’t scale with temperature.

The workflow for computing the quantum vibrational spectrum of a system using PIGS and the T_e *ansatz* can be summarized as follow. First, we perform short PIMD simulations exploring a range of temperatures and select the *lowest* temperature T_e by checking for

the alignment between the centroid and the physical radial distributions. Then, we use Eqs. (6) and (7) to machine-learn the centroid FES at β_e as a sum of local atom-centered components. In the final step, we predict quantum dynamical properties by performing MD at the desired temperatures. These simple steps enable the development of an effective PES that includes quantum nuclear effects for dynamics – an FES trained on a *single* high-temperature PI trajectory – and that is *transferable* across temperature. The computational details of all the simulations are described in sections I.B, I.D, and I.E of the SI.

We demonstrate the capabilities of the T_e PIGS approach by applying it to the IR spectrum of a water molecule – a challenging system that exhibits a strong red-shift of the stretching modes due to zero-point motion and a fine temperature-dependent splitting of the vibrational peaks due to the coupling of rotations and vibrations. We study the IR spectrum at 150 K, 300 K, and 600 K using the well-known Partridge-Schwenke model,⁵¹ which exhibits spectroscopic accuracy, and compare with experimental and numerically exact results.⁵³ We also compare with state-of-the-art approaches like CMD and thermostatted ring polymer molecular dynamics (TRPMD).¹⁸

The water molecule resides in its vibrational ground

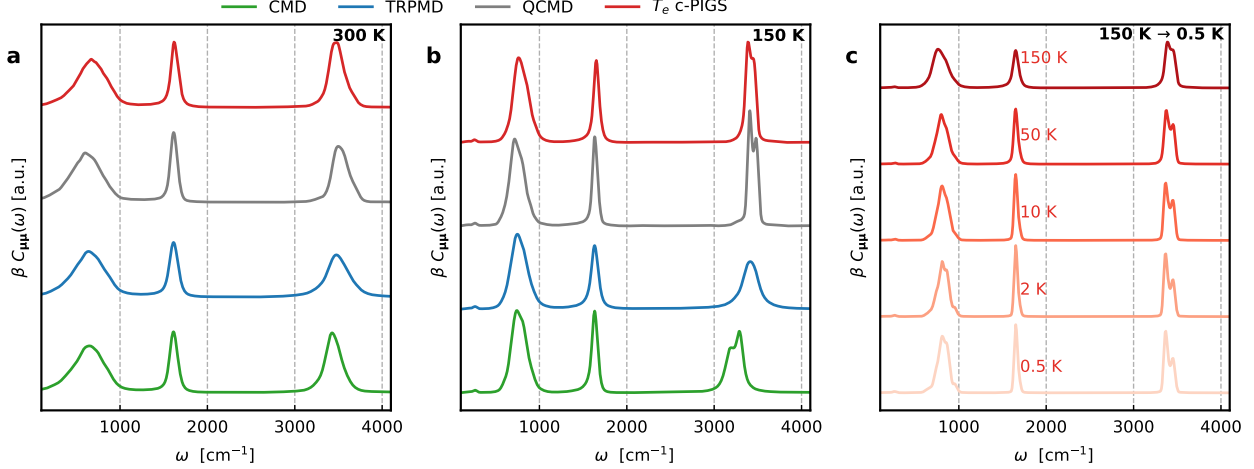


FIG. 4. **Quantum dynamics of bulk water.** Comparison of the vibrational spectrum of (a) liquid water at 300 K and (b) hexagonal ice at 150 K, described by a q-TIP4P/f⁵² water model, calculated using QCMD in black, the proposed T_e PIGS approach using the centroid free energy surface calculated at 600 K in red, CMD in blue, and TRPMD in green. Panel (c) displays the T_e PIGS IR spectrum predictions for hexagonal ice from 150 K down to 0.5 K.

state at least up to 600 K, but exhibits a sensitive dependence of the ro-vibrational splitting of the modes with temperature, as seen from the numerically exact IR spectra²⁸ in Fig. 3. The TRPMD approach largely captures the correct line positions of the (envelopes of) the stretching and the bending bands but is artificially broadened.¹⁸ The CMD approach gives a good description of the full IR spectrum at 600 K but is artificially red-shifted at 300 K and 150 K due to the onset of the curvature problem. This is confirmed by observing in Fig. 3 that the centroid distributions at 300 K and 150 K indicate a lower (unphysical) O-H bond length and misalignment with the physical radial distribution. Nevertheless, at 600 K we do not observe any “symptoms” of the curvature problem, and thus we use $T_e = 600$ K for the T_e PIGS approach.

As shown in Fig. 3, T_e PIGS spectra at 600 K are in excellent agreement with the exact and the independent CMD results, underlying the accuracy of the learned FES. More importantly, T_e PIGS describes the fundamental frequencies and the rotational splittings of the stretching and the bending modes at 300 K and 150 K, a substantial improvement over state-of-the-art PI methods in terms of accuracy. Furthermore, T_e PIGS is computationally efficient since this FES is estimated from a 100 ps PI trajectory with 8 replicas and a timestep of 0.5 fs, suggesting computational gains of at least a factor of 50×, 100× and 200× at 600 K, 300 K and 150 K, respectively, compared to a 100 ps long CMD simulations (without taking into account the higher sampling efficiency of T_e PIGS). To showcase the absence of computational scaling with temperature, we calculate the IR spectrum of a water molecule down to 0.5 K. Decrease in temperature expectedly reduces the

rotational splitting of the vibrational modes, and below 10 K, the system falls into its rotational ground state with well resolved peaks for the three vibrational modes. This temperature is in excellent agreement with the experimentally known rotational constants of a water molecule, i.e. 13–35 K.⁵⁴ Furthermore, the frequencies of the ground state vibrational bending mode matches the experimental / exact results⁵³ up to 8 cm^{−1} – the resolution of calculated spectra – and those of the two stretching modes are expectedly blue-shifted by around 40 cm^{−1} in excellent agreement with the results obtained from Mastubara dynamics²² – the true reference for PI based dynamical methods. We emphasize that the calculation of quantum mechanical spectrum at cryogenic temperatures by means of classical dynamics at this level of accuracy-to-cost ratio is unprecedented to our knowledge.

As a final test of our approach, we study the IR spectrum of condensed phase aqueous systems: bulk water at 300 K and hexagonal ice at 150 K. The presence of inter-molecule or crystal modes that couple with high-frequency modes should constitute a challenge for T_e PIGS as it has been the case with previous PI approaches.^{25,26} An additional challenge is that ice melts below the onset temperature of the curvature problem which could complicate the calculation of the FES at β_e . To circumvent this issue, we exploit the local nature of the FES (see Eq. 6) and insights from deep inelastic neutron scattering experiments⁷ that probe the quantum nuclear motion of atoms. These experiments suggest that the local potential felt by the nuclei due to quantum delocalization is short ranged⁵⁵ and sensitive/unique to their local environments.⁵⁶ Given that Eq. 6 makes the fitted FES size-extensive and local environments

of H and O atoms in ice are present in liquid water,⁵⁷ we conjecture that the T_e FES of hexagonal ice can be constructed from a high-temperature simulation of liquid water. We estimate vibrational spectra using the q-TIP4P/f water potential⁵² and a linear dipole moment surface. Although this model doesn't exhibit “experimental” or “spectroscopic” accuracy, it has been extensively used for comparing the performance of various PI^{19,28,35,58} and wavefunction-based^{11,12} methods and exhibits good agreement with the experimental spectra when combined with an appropriate dipole moment surface.⁵⁹

As shown in Fig. 4, we obtain well resolved spectra for both liquid water at 300 K and hexagonal ice at 150 K using a $T_e = 600$ K k_B FES fitted on a 10 ps PI simulation of liquid water. Our results are in good agreement with CMD, TRPMD and QCMD for room-temperature liquid water, where the curvature problem is small.³³ In the case of hexagonal ice at 150 K, we see a quantitative and qualitative improvement on the description of the high frequency band with respect to CMD and TRPMD and an excellent agreement with QCMD.²⁸ In addition to the increased accuracy, our approach is over three orders of magnitude less expensive (as measured by the number of force evaluations) than state-of-the-art approaches at 300 K and 150 K. Furthermore, the absence of temperature-dependent scaling behaviour of the cost, allows us to also compute the IR spectrum of hexagonal ice all the way down to 0.5 K. As expected, we observe that the system resides in its ground state and does not exhibit any line shifts of the high frequency modes.

In summary, we propose a new approach, T_e PIGS to simulate the quantum dynamics of light nuclei at the cost of classical MD. We use a physically-motivated temperature elevation *ansatz* that moves the system on the centroid FES obtained at a high temperature, and fitted efficiently by using machine-learning-based coarse-graining approaches.^{38–40} The T_e *ansatz* is exact in the high-frequency harmonic limit where the vibrational mode essentially lives in its ground state, as well as for low-frequency modes for which the ring polymer distribution collapses on the centroid. Furthermore, our study of condensed aqueous phases water shows that it also performs well for intermediate frequencies $\hbar\omega \sim \beta^{-1}$, for instance, the librational / rotational modes. These limits suggest that our approach could be useful for studying a wide range of systems with high-frequency modes that exhibiting weak coupling to rest of the system. We show that the T_e PIGS FES is *transferable* across temperatures and phases,

but is also size extensive, meaning that it allows for further computational savings by learning the FES on a smaller system. We believe that our approach constitutes a substantial improvement in accuracy over routinely used state-of-the-art methods like CMD and TRPMD. In addition, its low computational cost and the absence of its scaling behavior with temperature allows for accurate the IR spectra predictions even at cryogenic temperatures – considered prohibitive with state-of-the-art methods. We believe that the simplicity, low cost and high accuracy of T_e PIGS could open up prospects for routine modeling of quantum-vibrational spectra of general systems and direct comparisons with experiments, often performed at low temperatures.⁶⁰

ACKNOWLEDGEMENTS

We thank Start Althorpe, George Trenins, Christoph Schran, Angelos Michaelides, and members of the Clementi's group at FU for insightful discussions and comments on the manuscript. We also thank George Trenins for sharing QCMD results. V.K. acknowledges funding from the Swiss National Science Foundation (SNSF) under Project P2ELP2_191678 and the Ernest Oppenheimer Fund, allocation of CPU hours by CSCS under Project ID s1000, and support from Churchill College, University of Cambridge. C.C. acknowledges funding from the Deutsche Forschungsgemeinschaft DFG (SFB/TRR 186, Project A12; SFB 1114, Projects B03 and A04; SFB 1078, Project C7; and RTG 2433, Project Q05), the National Science Foundation (CHE-1738990, CHE-1900374, and PHY-2019745), and the Einstein Foundation Berlin (Project 0420815101). F.N. acknowledges funding from the Deutsche Forschungsgemeinschaft DFG (SFB 1114, Projects A04 and B08), The Berlin Mathematics center MATH+ (Projects AA1-6, AA2-8), The Berlin Institute for the Foundations of Learning Data (BIFOLD) and the European Commission (ERC CoG 772230). F.M. acknowledges support from the SNSF under the Postdoc.Mobility fellowship P500PT_203124 and from the Physics department at FU Berlin for the computational time.

SOURCE DATA

All the raw data and code required to reproduce the results, and scripts and raw data needed to make the figures is made available in the online repository: venkatkapil24/pigs-methodology.

[1] K. N. Houk and F. Liu, *Accounts of Chemical Research* **50**, 539 (2017).

[2] L. Pereyaslavets, I. Kurnikov, G. Kamath, O. Butin, A. Illarionov, I. Leontyev, M. Olevanov, M. Levitt, R. D.

Kornberg, and B. Fain, *Proceedings of the National Academy of Sciences* **115**, 8878 (2018).

[3] M. Benoit, D. Marx, and M. Parrinello, *Nature* **392**, 258 (1998).

[4] J. R. Cendagorta, H. Shen, Z. Bačić, and M. E. Tuckerman, *Advanced Theory and Simulations* **4**, 2000258 (2021).

[5] M. Liu, L. Zhang, M. A. Little, V. Kapil, M. Ceriotti, S. Yang, L. Ding, D. L. Holden, R. Balderas-Xicohténcatl, D. He, R. Clowes, S. Y. Chong, G. Schütz, L. Chen, M. Hirscher, and A. I. Cooper, *Science* **366**, 613 (2019).

[6] Y. Litman, J. O. Richardson, T. Kumagai, and M. Rossi, *Journal of the American Chemical Society* **141**, 2526 (2019).

[7] C. J. Burnham, G. F. Reiter, J. Mayers, T. Abdul-Redah, H. Reichert, and H. Dosch, *Physical Chemistry Chemical Physics* **8**, 3966 (2006).

[8] M. Rossi, W. Fang, and A. Michaelides, *The Journal of Physical Chemistry Letters* **6**, 4233 (2015).

[9] G. Li and H. Guo, *Journal of Molecular Spectroscopy* **210**, 90 (2001).

[10] H. R. Larsson, M. Schröder, R. Beckmann, F. Brieuc, C. Schran, D. Marx, and O. Vendrell, “State-resolved infrared spectrum of the protonated water dimer: Revisiting the characteristic proton transfer doublet peak,” (2022), arXiv:2206.12029 [physics, physics:quant-ph].

[11] Y. Wang and J. M. Bowman, *The Journal of Chemical Physics* **134**, 154510 (2011).

[12] S. M. Gruenbaum, C. J. Tainter, L. Shi, Y. Ni, and J. L. Skinner, *Journal of Chemical Theory and Computation* **9**, 3109 (2013).

[13] C. Qu, P. L. Houston, R. Conte, A. Nandi, and J. M. Bowman, *The Journal of Physical Chemistry A* **125**, 5346 (2021).

[14] S. C. Althorpe, *The European Physical Journal B* **94**, 155 (2021).

[15] T. E. Markland and M. Ceriotti, *Nature Reviews Chemistry* **2**, 1 (2018).

[16] J. Cao and G. A. Voth, *The Journal of Chemical Physics* **100**, 5106 (1994).

[17] I. R. Craig and D. E. Manolopoulos, *The Journal of Chemical Physics* **121**, 3368 (2004).

[18] M. Rossi, M. Ceriotti, and D. E. Manolopoulos, *The Journal of Chemical Physics* **140**, 234116 (2014).

[19] V. Kapil, D. M. Wilkins, J. Lan, and M. Ceriotti, *The Journal of Chemical Physics* **152**, 124104 (2020).

[20] T. J. H. Hele, M. J. Willatt, A. Muolo, and S. C. Althorpe, *The Journal of Chemical Physics* **142**, 134103 (2015).

[21] O. Marsalek and T. E. Markland, *The Journal of Physical Chemistry Letters* **8**, 1545 (2017).

[22] G. Trenins and S. C. Althorpe, *The Journal of Chemical Physics* **149**, 014102 (2018), publisher: American Institute of Physics.

[23] A. Witt, S. D. Ivanov, M. Shiga, H. Forbert, and D. Marx, *The Journal of Chemical Physics* **130**, 194510 (2009).

[24] F. Uhl, D. Marx, and M. Ceriotti, *The Journal of Chemical Physics* **145**, 054101 (2016).

[25] M. Rossi, V. Kapil, and M. Ceriotti, *The Journal of Chemical Physics* **148**, 102301 (2017).

[26] M. J. Willatt, M. Ceriotti, and S. C. Althorpe, *The Journal of Chemical Physics* **148**, 102336 (2018).

[27] J. Liu, *The Journal of Chemical Physics* **140**, 224107 (2014).

[28] G. Trenins, M. J. Willatt, and S. C. Althorpe, *The Journal of Chemical Physics* **151**, 054109 (2019).

[29] V. Kapil, J. VandeVondele, and M. Ceriotti, *The Journal of Chemical Physics* **144**, 054111 (2016).

[30] S. Shepherd, J. Lan, D. M. Wilkins, and V. Kapil, *The Journal of Physical Chemistry Letters* , 9108 (2021).

[31] T. Fletcher, A. Zhu, J. E. Lawrence, and D. E. Manolopoulos, *The Journal of Chemical Physics* **155**, 231101 (2021).

[32] D. Chandler and P. G. Wolynes, *The Journal of Chemical Physics* **74**, 4078 (1981).

[33] T. D. Hone, P. J. Rossky, and G. A. Voth, *The Journal of Chemical Physics* **124**, 154103 (2006).

[34] T. E. Markland and D. E. Manolopoulos, *The Journal of Chemical Physics* **129**, 024105 (2008).

[35] R. L. Benson, G. Trenins, and S. C. Althorpe, *Faraday Discussions* **221**, 350 (2019).

[36] C. Haggard, V. G. Sadhasivam, G. Trenins, and S. C. Althorpe, *The Journal of Chemical Physics* **155**, 174120 (2021).

[37] T. D. Hone, S. Izvekov, and G. A. Voth, *Journal of Chemical Physics* **122**, 054105 (2005).

[38] J. Wang, S. Olsson, C. Wehmeyer, A. Pérez, N. E. Charron, G. de Fabritiis, F. Noé, and C. Clementi, *ACS Central Science* **5**, 755 (2019).

[39] B. E. Husic, N. E. Charron, D. Lemm, J. Wang, A. Pérez, M. Majewski, A. Krämer, Y. Chen, S. Olsson, G. de Fabritiis, F. Noé, and C. Clementi, *J. Chem. Phys.* **153**, 194101 (2020).

[40] J. Wang, S. Chmiela, K.-R. Müller, F. Noé, and C. Clementi, *J. Chem. Phys.* **152**, 194106 (2020).

[41] F. Musil, A. Grisafi, A. P. Bartók, C. Ortner, G. Csányi, and M. Ceriotti, *Chemical Reviews* **121**, 9759 (2021), arXiv:2101.04673.

[42] O. T. Unke, S. Chmiela, H. E. Sauceda, M. Gastegger, I. Poltavsky, K. T. Schütt, A. Tkatchenko, and K. R. Müller, “Machine Learning Force Fields,” (2021), arXiv:2010.07067.

[43] S. Izvekov and G. A. Voth, *Journal of Chemical Physics* **123**, 134105 (2005).

[44] W. G. Noid, J. W. Chu, G. S. Ayton, V. Krishna, S. Izvekov, G. A. Voth, A. Das, and H. C. Andersen, *Journal of Chemical Physics* **128**, 244114 (2008).

[45] J. Wang, N. Charron, B. Husic, S. Olsson, F. Noé, and C. Clementi, *Journal of Chemical Physics* **154**, 164113 (2021).

[46] A. P. Bartók, R. Kondor, and G. Csányi, *Physical Review B* **87**, 184115 (2013), arXiv:1209.3140v2.

[47] J. P. Darby, J. R. Kermode, and G. Csányi (2021) arXiv:2112.13055.

[48] F. Musil, M. Veit, A. Goscinski, G. Fraux, M. J. Willatt, M. Stricker, T. Junge, and M. Ceriotti, *Journal of Chemical Physics* **154**, 114109 (2021), arXiv:2101.08814.

[49] V. Kapil, M. Rossi, O. Marsalek, R. Petraglia, Y. Litman, T. Spura, B. Cheng, A. Cuzzocrea, R. H. Meißner, D. M. Wilkins, B. A. Helfrecht, P. Juda, S. P. Binenvenue, W. Fang, J. Kessler, I. Poltavsky, S. Vandenbrande, J. Wieme, C. Corminboeuf, T. D. Kühne, D. E. Manolopoulos, T. E. Markland, J. O. Richardson, A. Tkatchenko, G. A. Tribello, V. Van Speybroeck, and M. Ceriotti, *Computer Physics Communications* **236**, 214 (2019).

[50] A. Paszke, S. Gross, F. Massa, A. Lerer, J. Bradbury, G. Chanan, T. Killeen, Z. Lin, N. Gimelshein, L. Antiga, A. Desmaison, A. Kopf, E. Yang, Z. DeVito, M. Raison, A. Tejani, S. Chilamkurthy, B. Steiner, L. Fang, J. Bai, and S. Chintala, in *Advances in Neural Information Processing Systems 32*, edited by H. Wallach, H. Larochelle, A. Beygelzimer, F. d'Alché-Buc, E. Fox, and R. Garnett (Curran Associates, Inc., 2019) pp. 8024–8035.

[51] H. Partridge and D. W. Schwenke, *The Journal of Chemical Physics* **106**, 4618 (1997).

[52] S. Habershon, T. E. Markland, and D. E. Manolopoulos, *The Journal of Chemical Physics* **131**, 024501 (2009).

[53] Z. Gao, N. Giovambattista, and O. Sahin, *Scientific Reports* **8**, 6228 (2018).

[54] R. T. Hall and J. M. Dowling, *The Journal of Chemical Physics* **47**, 2454 (1967).

[55] L. Lin, J. A. Morrone, R. Car, and M. Parrinello, *Physical Review Letters* **105**, 110602 (2010).

[56] C. Andreani, G. Romanelli, and R. Senesi, *The Journal of Physical Chemistry Letters* **7**, 2216 (2016).

[57] P. Gasparotto, R. H. Meißner, and M. Ceriotti, *Journal of Chemical Theory and Computation* **14**, 486 (2018).

[58] M. Rossi, H. Liu, F. Paesani, J. Bowman, and M. Ceriotti, *The Journal of Chemical Physics* **141**, 181101 (2014).

[59] H. Liu, Y. Wang, and J. M. Bowman, *The Journal of Physical Chemistry B* **120**, 1735 (2016).

[60] D. Verma, R. M. P. Tanyag, S. M. O. O'Connell, and A. F. Vilesov, *Advances in Physics: X* **4**, 1553569 (2019).

Supporting Information: Quantum dynamics using path integral coarse-graining

Félix Musil,¹ Iryna Zaporozhets,^{1,2,3} Frank Noé,^{1,3,2}

Cecilia Clementi,^{1,3,2,*} and Venkat Kapil^{4,†}

¹*Department of Physics, Freie Universität Berlin,
Arnimallee 12, 14195 Berlin, Germany*

²*Department of Chemistry, Rice University,
Houston, Texas 77005, United States*

³*Center for Theoretical Biological Physics,
Rice University, Houston, Texas 77005, United States*

⁴*Yusuf Hamied Department of Chemistry, University of Cambridge,
Lensfield Road, Cambridge, CB2 1EW, UK*

* cecilia.clementi@fu-berlin.de

† vk380@cam.ac.uk

I. COMPUTATIONAL DETAILS

A. DVR calculations

The 2D radial Morse potential mimicking the O–H bond, as described in the main text is defined as

$$\hat{H} = (2\mu)^{-1} [\hat{p}_x^2 + \hat{p}_y^2] + D \left[1 - e^{-\alpha(\sqrt{\hat{q}_x^2 + \hat{q}_y^2} - r_0)} \right]^2, \quad (1)$$

with $\mu = 1741.1$ a.u. the reduced mass of O and H atoms, $D = 0.18748$ a.u. the bond dissociation energy, $r_0 = 1.8324$ a.u. is the bond length parameter and $\alpha = 1.1605$ a.u. a parameter describing the the anharmonicity along the bond. We solved the time-independent Schrödinger’s equation using sinc-function discrete variable representation¹ implemented in Nuclear Solver². The potential was solved on a grid with dimensions $x = [-6.0, 6.0]$ a.u. and $y = [-6.0, 6.0]$ a.u. using a uniform grid with 400 points in each direction. These parameters yield converged values for at least the first 32 eigenvalues.

B. PIMD simulations

We performed PIMD simulations of all systems in the canonical ensemble using the PILE-L and PILE-G thermostats³ of time constants 100 fs for building the datasets used to train the machine learning models. We used a timestep of 0.5 fs and integrated the PI equations of motion using a BAOAB splitting⁴ of the Liouville operator. We sampled the centroid positions and forces every 10 fs. Simulations were run for 100 ps at temperatures $\{100 \text{ K}, 200 \text{ K}, \dots, 900 \text{ K}, 1000 \text{ K}\}$ using 64 replicas at all temperatures using the i-PI code⁵.

C. ML model

We model the atomic potential of mean force, A_a , by representing the atomic environment with the normalized SOAP power spectrum^{6,7} and pass these 3-body features to multi-layer perceptron with 3 hidden layers of width [400, 200, 200] and the hyperbolic tangent activation function. The SOAP features are defined by:

$$p_{a_1 a_2 n_1 n_2 l}^{(i)} = \sum_m (-1)^m c_{a_1 n_1 l m}^{(i)} c_{a_2 n_2 l (-m)}^{(i)}, \quad (2)$$

where

$$c_{anlm}^{(i)} = \sum_{(j,b) \in i} \delta_{ab} R_{nl}(r_{ij}) Y_l^m(\hat{\mathbf{r}}_{ij}) f_c(r_{ij}) \quad (3)$$

are the spherical expansion coefficients associated with atom i , the sum runs over the neighbors j of species b of atom i , R_{nl} is a radial basis function, Y_l^m are spherical harmonics functions, f_c is a smooth cutoff function of radius r_c , $\mathbf{r}_{ij} = \mathbf{r}_j - \mathbf{r}_i$ is the separation vector going from the central atom i to the neighbor atom j , $r_{ij} = \|\mathbf{r}_{ij}\|$ is its length, and $\hat{\mathbf{r}}_{ij} = \mathbf{r}_{ij}/r_{ij}$ is its direction. The basis expansion in Eq. (3) is truncated up to $n < 12$ radial channels and $l \leq 6$ angular channels. Furthermore, R_n is the splined GTO radial integral⁷ with $\sigma = 0.3$, the cutoff radius is $r_c = 3 \text{ \AA}$, and the number of SOAP features is reduced by using a lossless compression scheme⁸. The parameters of the multi layer perceptron are optimized using the LAMB⁹ ($l_r = 0.001$, $\beta = (0.9, 0.999)$) and stochastic weight averaging¹⁰.

D. CMD simulations

We performed partially adiabatic CMD simulations¹¹ of all systems in the canonical ensemble using a weak PILE-G thermostat³ of time constants 1000 fs and a Parrinello-Rahman mass matrix¹² to rescale the non-centroid frequencies to 13000 cm⁻¹. We used a timestep of 0.01 fs and integrated the PI equations of motion using an OBABO splitting⁴ of the Liouville operator. We sampled the centroid positions every 0.25 fs. Simulations were run for 100 ps at temperatures 150 K, 300 K and 600 K using 64, 32, and 160 replicas, respectively, using the i-PI code⁵.

E. MD / TRPMD simulations and PIGS

We performed partially adiabatic TRPMD simulations¹¹ of all systems in the canonical ensemble using a PILE-G thermostat³ of time constants 100 fs and PILE- $\lambda=0.5$. We used a timestep of 0.25 fs and integrated the PI equations of motion using an OBABO splitting⁴ of the Liouville operator. We sampled the bead positions every 0.25 fs. Simulations were run for 100 ps at temperatures 150 K, 300 K and 600 K using 64, 32, and 160 replicas, respectively, using the i-PI code⁵.

MD simulations and PIGS were performed by setting the number of replicas to one. Note that the simulations used to compute the IR spectra of water have been performed in two steps in order to sample the system sufficiently. First an NVT simulation with the Langevin thermostat was performed from which 100 configurations were sampled randomly to start NVT simulations with a weak stochastic velocity rescaling thermostat¹³ simulations – known to improve sampling without significantly perturbing the dynamics of the system³.

II. THE TEMPERATURE ELEVATION ANSATZ

A. Ground state quantum time correlation function

The standard time correlation function (TCF) of operators \hat{A} and \hat{B} for a Hamiltonian \hat{H} at an inverse temperature $\beta = k_B T$ is

$$c_{\hat{A}\hat{B}}(t) = Z^{-1} \operatorname{Tr} \left[e^{-\beta\hat{H}} \hat{A} e^{i\hbar^{-1}\hat{H} t} \hat{B} e^{-i\hbar^{-1}\hat{H} t} \right], \quad (4)$$

where Z is the canonical partition function of the system. One can rewrite Eq. 4 by computing the trace in the basis of the eigenstates of H , and inserting a resolution of identity

$$c_{\hat{\mu}\hat{\mu}}(t) = Z^{-1} \sum_{j,k} e^{-\beta E_j} \langle j | \hat{A} | k \rangle \langle k | \hat{B} | j \rangle e^{i\hbar^{-1}(E_k - E_j) t} \quad (5)$$

with $\hat{H} |i\rangle = E_i |i\rangle$. The Fourier transform of the TCF is

$$C_{\hat{A}\hat{B}}(\omega) = Z^{-1} \sum_{j,k} e^{-\beta E_j} \langle j | \hat{A} | k \rangle \langle k | \hat{B} | j \rangle \delta(\omega - \hbar^{-1}(E_k - E_j)). \quad (6)$$

For a system in the ground state, i.e., $\hbar\omega \gg \beta^{-1}$, and thus the Boltzmann weight of the excited vibrational states can be ignored. Eq. 6 can be rewritten as a temperature-independent sum over matrix elements of the dipole operator:

$$C_{\hat{A}\hat{B}}(\omega) \approx \sum_k \langle j | \hat{A} | k \rangle \langle k | \hat{B} | j \rangle \delta(\omega - \hbar^{-1}(E_k - E_j)) \quad (7)$$

The corresponding Kubo-transformed TCF $\tilde{C}_{\hat{A}\hat{B}}(\omega)$ is linked by the harmonic detailed balance relation $C_{\hat{\mu}\hat{\mu}}(\omega) = \tilde{C}_{\hat{\mu}\hat{\mu}}(\omega) \frac{\beta\hbar\omega}{1 - e^{-\beta\beta\hbar\omega}}$. For a system in the ground state

$$\beta\tilde{C}_{\hat{A}\hat{B}}(\omega) \approx (\hbar\omega)^{-1} \sum_k \langle j | \hat{A} | k \rangle \langle k | \hat{B} | j \rangle \delta(\omega - \hbar^{-1}(E_k - E_j)). \quad (8)$$

B. Choice of T_e

The choice of T_e depends on the anharmonicity of the system as T_e should be large enough to alleviate the curvature problem but small enough for the harmonic approximation to be valid. For instance, for a harmonic system, an arbitrarily large T_e is a suitable as the classical and the quantum *fundamental* transition frequencies are equal. On the other hand, for anharmonic systems, there is a need to select a low enough T_e as the $T_e \rightarrow \infty$ limit yields the (oft blue-shifted) classical line position. As discussed in the main text, an easy and robust approach for selecting a T_e is by comparing the alignment of the centroid and the physical probability distributions.

As shown in Fig. 1, the T_e dependence of the fundamental transition frequency displays three distinct regimes. The curvature problem is attenuated for $T_e < 400$ K and beyond 600 K, anharmonic effects lead to a systematic blue shift to the classical transition frequency at $T_e \rightarrow \infty$. We observe a *goldilocks scenario* in the temperature range, 400 K to 600 K, where the curvature problem is cured and anharmonic effects are small; any T_e in this range of temperature should be a valid choice.

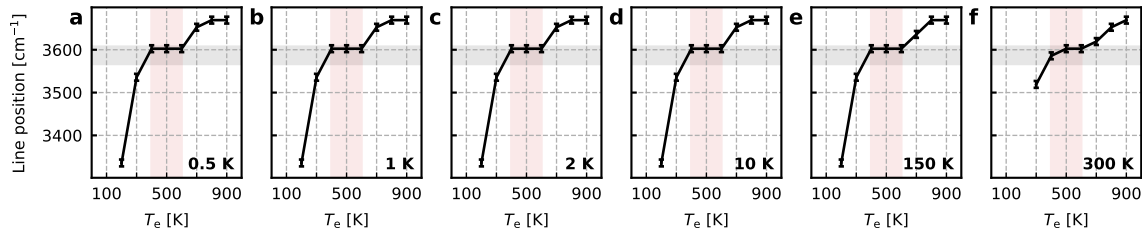


FIG. 1. Dependence of the line position of a 2D Morse oscillator on T_e . The black shaded region shows the range between frequencies obtained by DVR (numerically exact) and Matsubara dynamics¹⁴. The red shaded region is used to indicate the range of suitable T_e values.

- [1] D. T. Colbert and W. H. Miller, [The Journal of Chemical Physics](#) **96**, 1982 (1992).
- [2] T. Graen and H. Grubmüller, [Computer Physics Communications](#) **198**, 169 (2016).
- [3] M. Ceriotti and D. E. Manolopoulos, [Physical Review Letters](#) **109**, 100604 (2012).

[4] V. Kapil, J. Wieme, S. Vandenbrande, A. Lamaire, V. Van Speybroeck, and M. Ceriotti, *Journal of Chemical Theory and Computation* **15**, 3237 (2019).

[5] V. Kapil, M. Rossi, O. Marsalek, R. Petraglia, Y. Litman, T. Spura, B. Cheng, A. Cuzzocrea, R. H. Meißner, D. M. Wilkins, B. A. Helfrecht, P. Juda, S. P. Bienvenue, W. Fang, J. Kessler, I. Poltavsky, S. Vandenbrande, J. Wieme, C. Corminboeuf, T. D. Kühne, D. E. Manolopoulos, T. E. Markland, J. O. Richardson, A. Tkatchenko, G. A. Tribello, V. Van Speybroeck, and M. Ceriotti, *Computer Physics Communications* **236**, 214 (2019).

[6] A. P. Bartók, R. Kondor, and G. Csányi, *Physical Review B* **87**, 184115 (2013), [arXiv:1209.3140v2](https://arxiv.org/abs/1209.3140v2).

[7] F. Musil, M. Veit, A. Goscinski, G. Fraux, M. J. Willatt, M. Stricker, T. Junge, and M. Ceriotti, *Journal of Chemical Physics* **154**, 114109 (2021), [arXiv:2101.08814](https://arxiv.org/abs/2101.08814).

[8] J. P. Darby, J. R. Kermode, and G. Csányi (2021) [arXiv:2112.13055](https://arxiv.org/abs/2112.13055).

[9] Y. You, J. Li, S. Reddi, J. Hseu, S. Kumar, S. Bhojanapalli, X. Song, J. Demmel, K. Keutzer, and C.-J. Hsieh, (2019), [10.48550/arxiv.1904.00962](https://arxiv.org/abs/1904.00962), [arXiv:1904.00962](https://arxiv.org/abs/1904.00962).

[10] P. Izmailov, D. Podoprikhin, T. Garipov, D. Vetrov, and A. G. Wilson, in *34th Conference on Uncertainty in Artificial Intelligence 2018, UAI 2018*, Vol. 2 (2018) pp. 876–885, [arXiv:1803.05407](https://arxiv.org/abs/1803.05407).

[11] T. D. Hone, P. J. Rossky, and G. A. Voth, *The Journal of Chemical Physics* **124**, 154103 (2006).

[12] M. Parrinello and A. Rahman, *The Journal of Chemical Physics* **80**, 860 (1984).

[13] G. Bussi, D. Donadio, and M. Parrinello, *The Journal of Chemical Physics* **126**, 014101 (2007).

[14] G. Trenins, M. J. Willatt, and S. C. Althorpe, *The Journal of Chemical Physics* **151**, 054109 (2019).